Microchimica Acta
https://doi.org/10.1007/s00604-017-2564-x

ORIGINAL PAPER

A gold electrode modified with a nanoparticulate film composed of a conducting copolymer for ultrasensitive voltammetric sensing of hydrogen peroxide

Rongli Zhang[1] · Can Jiang[1] · Xiaoxia Fan[2] · Renchun Yang[1] · Yanyan Sun[1] · Cuige Zhang[1]

Received: 16 August 2017 / Accepted: 9 November 2017

Abstract
A film consisting of poly(γ-glutamic acid) modified with 3-aminothiophene (ATh-γ-PGA) was prepared by macromolecular self-assembly and electropolymerization. ATh-γ-PGA is amphiphilic and electrically conductive. The copolymers undergo self-assembly to form nanoparticles (NPs) on decreasing the pH value of an aqueous solution. A conducting film of NPs was formed on the surface of a gold electrode by casting the ATh-γ-PGA NPs and subsequently electropolymerizing the thiophene units. Next, horseradish peroxidase and Nafion were cast onto the film to obtain an enzymatic biosensor for H_2O_2. Due to the electropolymerization step, a cross-conjugated polymer network is created that improves electron transfer rates and thus enhances the response. This endows the biosensor with high sensitivity. Two linear ranges are present, the first ranging from 1×10^{-11} to 1×10^{-8} mol·L^{-1}, and the second from 1×10^{-8} to 1×10^{-5} mol·L^{-1}. The detection limit is as low as 3×10^{-12} mol·L^{-1}. The sensor is stable, repeatable, and was successfully applied to the determination of H_2O_2 in a commercial disinfecting solution.

Keywords 3-Aminothiophene · Poly(γ-glutamic acid) · Macromolecular assembly · Electropolymerization · Biosensor

Introduction

Hydrogen peroxide (H_2O_2) is an excellent cleaning agent or bleaching, which is often used in clinical, biological, environmental and many other fields [1]. It is urgent to find a sensitive determination method for H_2O_2. Many materials have been used to immobilize enzyme on the electrode surface to prepare biosensor for detecting H_2O_2, such as quantum dots [2], polymers [3], mesoporous materials [4] and nanomaterials [5]. Among these materials, biocompatible nanomaterials are competitive candidates due to their unique advantages such as large high surface reaction activity, strong adsorption ability, surface-to volume-ratio and high-catalytic activity for enzyme immobilization [6]. Furthermore, biocompatible nanomaterials-based enzyme biosensor renders the microenvironment for keeping biological activity and enhancing the direct electron transfer (DET) between the active sites of enzymes and the electrode [7, 8].

Self-assembled nanoparticles (NPs) prepared from amphiphilic copolymer including various morphologies (such as spheres, rods, bowls and vesicles) have attracted much attention. Combined the nanoscale effects and/or fascinating structures, the self-assembled NPs are useful in many potential applications, such as sensors, drug delivery, catalysts and others [9–14]. Miao et al. [6] used botanical inositol hexakisphosphoric NPs to immobilize horseradish peroxidase (HRP) for preparing enzyme-based biosensor. The prepared biosensor for H_2O_2 sensing exhibited a low detection limit and a long-term stability. In our previous work, a kind of photosensitive amphiphilic poly(γ-glutamic acid)-*graft*-7-amino-4-

Electronic supplementary material The online version of this article (https://doi.org/10.1007/s00604-017-2564-x) contains supplementary material, which is available to authorized users.

✉ Rongli Zhang
zrl326@163.com

✉ Cuige Zhang
zcg17131@ahpu.edu.cn

[1] School of Biological and Chemical Engineering, Anhui Polytechnic University, Wuhu 241000, China

[2] Xi'an North Huitian Chemical Industry Co. Ltd., Xi'an 710302, China

Published online: 18 December 2017

methylcoumarin NPs was used as a matrix to entrap and immobilize hemoglobin (Hb) on electrode surface to prepare biosensor [15]. The subsequent photo-crosslinking locked Hb in NPs film. The resultant biosensor showed good biocatalytic activity for H_2O_2. The biocompatible self-assembled NPs can increase the loading of electroactive species for signal amplification. The modified electrode formed by self-assembled NPs platform has the advantages of high uniformity and organization, which provides excellent microenvironment for enzyme immobilization and facilitates DET from the electroactive enzyme to the underlying electrode. However, due to the self-assembled NPs prepared from non-conducting biopolymer, the electron transfer between NPs film and underlying electrode was slow, which greatly limited its detection limit and sensitivity.

Polythiophene is an important class of conjugated conducting polymers, which has potential application in sensors and biosensors [16–18]. In this work, a novel kind of conducting NPs film prepared by self-assembly of an electroactive amphiphilic 3-aminothiophene modified poly(γ-glutamic acid) (ATh-γ-PGA) copolymer and electropolymerization was employed to construct a electrochemical biosensor for voltammetric sensitive sensing H_2O_2. The whole strategy is depicted in Fig. 1. First, the electroactive ATh-γ-PGA was synthesized via amidation reaction. The amphiphilic ATh-γ-PGA copolymer assembled into NPs in aqueous solution through decreasing the pH value of solution. Then, the ATh-γ-PGA NPs were cast onto the surface of gold electrode (GE) to form a NPs film. The subsequent electropolymerization of the electroactive thiophene units in NPs film created cross-conjugated polymer network, which enhanced the conductivity of the ATh-γ-PGA NPs film. After HRP and Nafion were cast on the NPs film, a biosensor was successfully fabricated. It is quite expected that the good conductivity of the in situ formed polythiophene network provides a platform to accelerate the electron transfer and facilitate the signal transduction from the NPs film to the GE, leading to high sensitivity of the electrochemical biosensor.

Experimental

Reagents and materials

Poly (γ-glutamic acid) (γ-PGA, Mw 700,000–100,000) was obtained from AMRESCO (USA, https://www.amresco-inc.com), 3-aminothiophene (ATh), Nafion, phosphate, horse radish peroxidase (HRP), HCl, $LiClO_4$, acetonitrile, H_2O_2, $K_3[Fe(CN)_6]$, KCl, $K_4[Fe(CN)_6]$, 1-(3-Dimethylaminopropyl)-3-ethylcarbodiimide hydrochloride (EDC·HCl) and N-hydroxysuccinimide (NHS), were supplied by Aladdin Chemistry Co. Ltd. (Shanghai, China, http://www.aladdin-e.com).

Synthesis of ATh-γ-PGA

ATh-γ-PGA was synthesized via amidation reaction between the carboxyl group of γ-PGA and amino group of 3-aminothiophene in the presence of EDC·HCl and NHS. Briefly, 2 mmol γ-PGA (repeat unit) was dissolved in 40 mL distilled water under stirring in an ice-bath. After 0.5 h, 2 mmol EDC·HCl and 4 mmol NHS were added into the resulted solution. After 5 min of stirring, 2 mmol 3-aminothiophene was added to the mixture. The reaction was carried out in an ice-bath for another hour and then at room temperature overnight. The ATh-γ-PGA copolymer was purified via dialysis using a dialysis membrane (MC: 14,000) in distilled water. Purification was considered to be completed when no free 3-aminothiophene was detectable in the wash solution by UV. Finally, the washed ATh-γ-PGA copolymer solution was frozen and then lyophilized. The synthetic route of ATh-γ-PGA copolymer is shown in Fig. S1.

Preparation and characterization of ATh-γ-PGA NPs

The ATh-γ-PGA copolymer, which contains thiophene moieties and —COO^- groups at the side chains, is an anionic polyelectrolyte with pH-responsiveness. After ATh-γ-PGA copolymer was dissolved in distilled water, aqueous HCl was used to adjust the pH value of the solution. With decreasing the pH value of solution, ATh-γ-PGA copolymer self-assembled into NPs. A volume of 10 mL of the ATh-γ-PGA solution was removed at different pH values and left for 2 h to equilibrate before the turbidity and size distribution measurements. The turbidity was calculated as turbidity = $1–10^{-A}$, where A is the absorbance of the ATh-γ-PGA solution with different pH values at 550 nm measured by TU-1901 UV–vis spectrophotometry [19].

Fabrication and characterization of the biosensor

A bare gold electrode (GE) was polished by alumina particles and washed by ethanol and distilled water under ultrasonication. The cleaned GE was then subjected to cyclic sweeping between −0.40 and 1.60 V in 1.0 $mol·L^{-1}$ H_2SO_4 until a stable cyclic voltammogram was obtained. 5 μL of the ATh-γ-PGA NPs solution was cast evenly onto the surface of GE and then dried on the air. After that, the electrode covered with At-γ-PGA NPs film (ATh-γ-PGA/GE) was subjected to electrochemical polymerization to induce the cross-linking of the thiophene group. Electrochemical polymerization was performed via cyclic voltammetry (CV) with the scan range of 0 to 1.5 V at a potential scan rate of 100 $mV·s^{-1}$ for 20 cycles in a

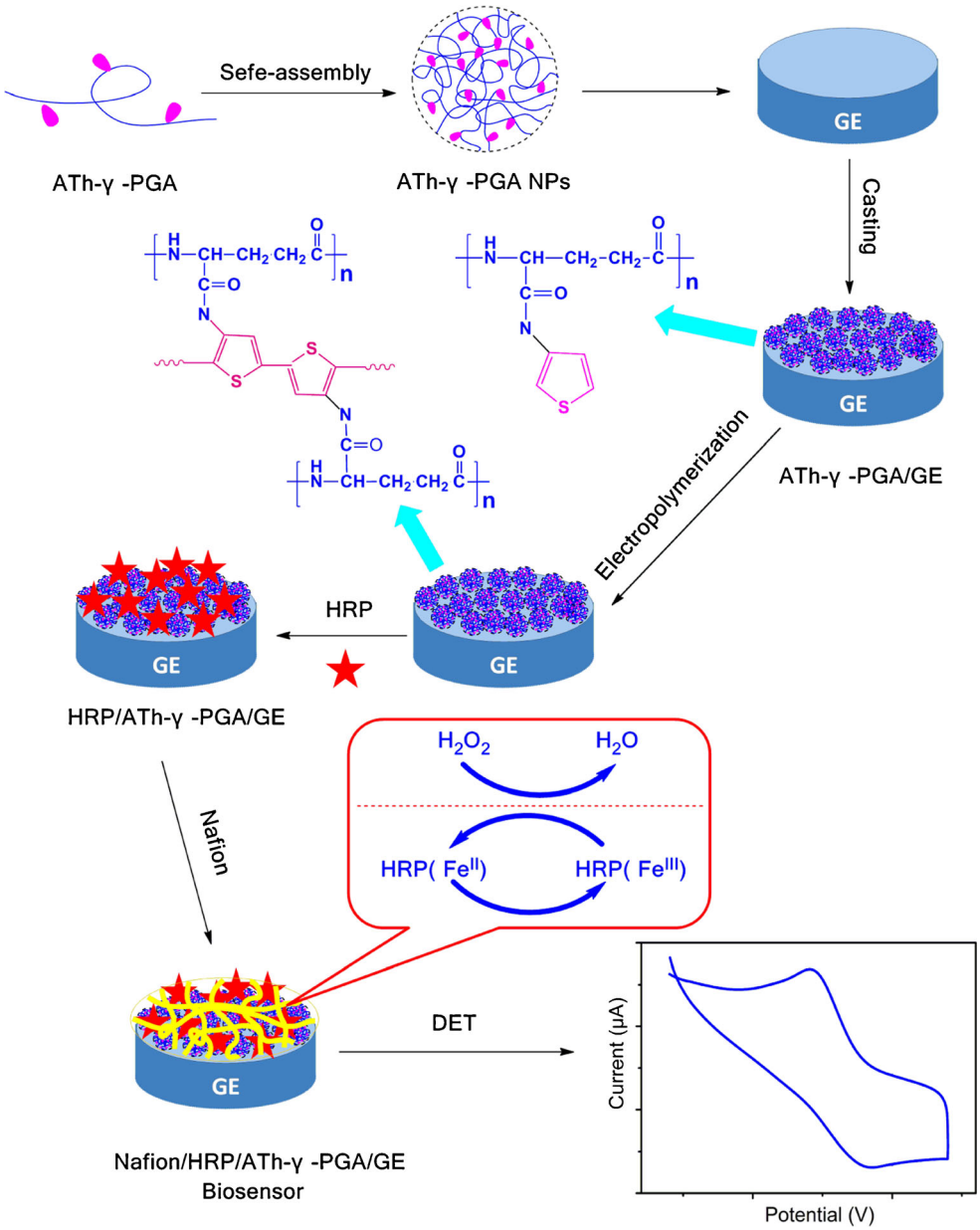

Fig. 1 Schematic illustration of the biosensor fabrication using the self-assembled electroactive ATh-γ-PGA NPs

solution of 0.1 mol·L^{-1} $LiClO_4$ dissolved in acetonitrile [20]. After that, 5 μL of the HRP solution (5 mg·mL^{-1}, pH 7.4 phosphate buffered saline (PBS) solution) was dropped onto the surface of ATh-γ-PGA/GE, which was dried in 4 °C about 12 h. And then, the electrode HRP/ATh-γ-PGA/GE was successively coated with 5 μL of the Nafion solution (five times diluted by pH 7.0 PBS solution). After thoroughly rinsing 3 times with distilled water to remove the physically adsorbed HRP, the Nafion/HRP/ATh-γ-PGA/GE biosensor was fabricated. It was storied at 4 °C in pH 7.0 PBS solution while not used. For comparison, Nafion/HRP/γ-PGA/GE was fabricated using the similar procedures.

Characterization and measurement

^{1}H NMR spectrum was recorded using a Bruker (400 MHz) instrument. Infrared (IR) experiment was run by attenuate total reflexion (ATR) mode on a Nicolet FI-IR Spectrometer instrument. Ultraviolet visible (UV–vis) spectra and UV Absorbance were recorded with a TU-1901 spectrophotometer (Beijing Purkinje General instrument Co., Ltd.). Solution pH value was monitored using a pHS-3C precision digital pH meter (Shanghai Precision & Scientific Instrument Co. Ltd.). The particle size and size distribution were measured using a Zeta PALS instrument (Brookhaven Instruments Corporation, Holtsville, USA). The morphology of NPs and the coated

electrodes were observed by a Hitachi S-4800 field emission scanning electron microscope (FESEM) operating at 2.0 kV. Transmission electron microscope (TEM) images were recorded in a JEOL JEM-2100 at 200 kV. All electrochemical experiments were performed using a CHI 660E electrochemical workstation with a three-electrode cell. The three electrode system included a saturated calomel electrode as reference electrode, a platinum wire electrode as counter electrode and the modified GE as the working electrode.

Results and discussion

Choice of material

Conducting polymers (polyaniline, polypyrrole, polythiophene, etc.) have attracted considerable interest in sensors and biosensors because of their attractive electrical, environmental stability, and as well as biocompatibility and conformability [21–24]. Providing many advantages such as enhanced biocatalytic stability, easy protection against the negative environmental impact, and allowed the application of modified electrodes in a wider range of experimental conditions, conducting polymers can be used as an immobilization matrix for biologically active molecules in biosensor [21, 22]. Among these conducting polymers, polythiophene has been often considered as a model for the study of charge transport in conducting polymers. Moreover, polythiophene shows the high environmental stability of both doped and undoped states together with theirs structural versatility [21, 22]. Herein, 3-aminothiophene was used to modify γ-PGA to prepare electroactive ATh-γ-PGA NPs.

Preparation and characterization of ATh-γ-PGA NPs

The preparation and characterization of the ATh-γ-PGA copolymer are shown in electronic supplementary material. With hydrophobic thiophene groups and hydrophilic —COO^- groups, the amphiphilic ATh-γ-PGA copolymer can self-assemble into NPs in aqueous solution by simply decreasing the pH value. The self-assembly behavior of ATh-γ-PGA copolymer was monitored through turbidity experiment [19]. The turbidities of 0.1 mg·mL^{-1} aqueous solutions of γ-PGA and ATh-γ-PGA copolymer at 550 nm as a function of solution pH are shown in Fig. S4. As can be seen, the turbidities of γ-PGA aqueous solution showed negligible changes from pH 5.60 to pH 1.50, indicating that no NPs were formed in this pH value range. In contrast, the turbidities of ATh-γ-PGA copolymer solution exhibited a clear break point at pH 2.5, indicating the formation of NPs at this pH value. The possible reason is that with the decrease of pH value, the protonation of the hydrophilic —COO^- groups makes ATh-γ-PGA more hydrophobic, leading to self-assembly of the copolymer and formation of the NPs. As pH value further decreased, the turbidities sharply increased. The significant increasing turbidity may be ascribed to the small NPs agglomerating to large particles, as a result of the weakening electrostatic repulsion between the NPs with further decreasing pH value. Below pH 2.00, macroscopic precipitation was observed. The sizes of ATh-γ-PGA NPs in solution with different pH values are shown in Fig. S5. As can be seen, the stable ATh-γ-PGA NPs formed at the range of pH 3.5~2.0. The size distributions of ATh-γ-PGA NPs formed at pH 2.5 are shown in Fig. 2. It can be seen, the size of ATh-γ-PGA NPs increased from 86.3, 96.2 to 103.7 with the increase of modification degree of ATh-γ-PGA from 16.3%, 19.3% to 22.0%.

With the highest modification degree, ATh-γ-$PGA_{22.0\%}$ NPs formed in solution at pH 2.5 were used in the following experiments. The morphology of ATh-γ-$PGA_{22.0\%}$ NPs was confirmed by TEM and SEM (shown in Fig. 3), which revealed a spherical morphology with an average diameter of 110 nm.

Fabrication and characterization of the biosensor

The prepared ATh-γ-$PGA_{22.0\%}$ NPs were then immobilized on GE surface via casting method to form NPs film. Electropolymerization was subsequently carried out owing to the existence of a large amount of thiophene groups in NPs film. Thiophene is a well-known electroactive moiety which can electropolymerize to create a large conjugated polythiophene structure [25]. The electropolymerization of thiophene moieties can form a conjugated conducting network containing both inter- and intramolecular crosslinkages between the pendant thiophene units (Fig. S6) throughout the ATh-γ-$PGA_{22.0\%}$ NPs film, which played important roles for the preparation of high-performance biosensor. With the formation of crossconjugated conductive polymer network, the electrical property of the NPs film was greatly enhanced, which can accelerate the electron transfer and facilitate the signal transduction from the enzyme to the electrode. Figure S7 shows typical CVs obtained by scanning electropolymerization from 0.0 and 1.5 V vs. SCE in a fresh acetonitrile solution of $LiClO_4$. In the first cycle, the onset of oxidation potential of thiophene units located at 1.41 V. Upon consecutive cycle, the onset of oxidation potential gradually decreased, revealing polymer was easier to oxidize than monomer [26]. The ATh-γ-$PGA_{22.0\%}$ NPs film after electropolymerization was then used as a biopolymeric NPs platform for immobilizing HRP to fabricate biosensor. The interfacial properties and morphologies of different modified electrodes were characterized by electrochemical impedance spectroscopy (EIS) and SEM, respectively.

EIS [27] is an effective method to monitor the interfacial properties of the modified electrodes. The typical impedance

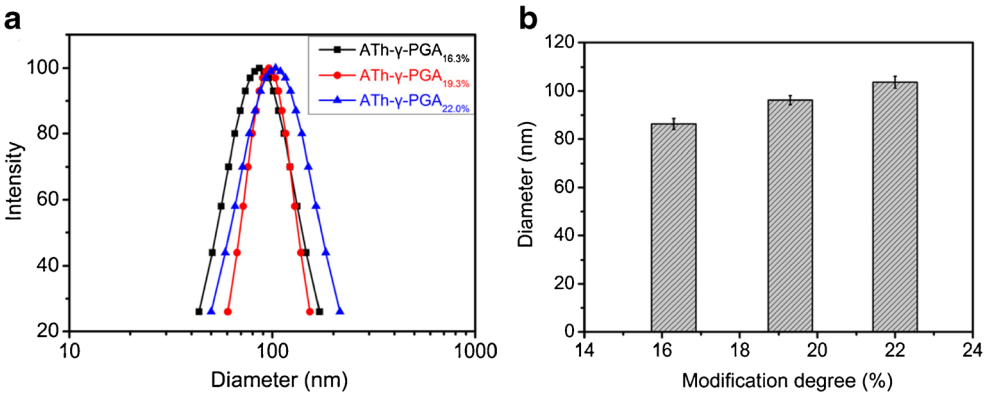

Fig. 2 Size distributions (**a**) and sizes (**b**) of ATh-γ-PGA NPs with different modification degrees formed in aqueous solution at pH 2.5. The concentration of the γ-PGA and ATh-γ-PGA aqueous solution was 0.1 mg·mL^{-1}

spectrum which is present in the form of a Nyquist plot includes two parts: the semicircular part at higher frequencies corresponds to the electron-transfer limiting process and the linear part at a lower frequency corresponds to the diffusion process. The diameter of semicircular part corresponds to the electron transfer resistance (R_{ct}) which controls the electron transfer kinetics of the redox probe (such as $[Fe(CN)_6]^{3-/4-}$) at the electrode interface. EIS was employed to characterize the interfacial properties of the electrodes with different modifications. To get an equilibrated situation at the electrode surface, the impedance spectra were recorded at an open-circuit voltage and an AC amplitude of 5 mV over a frequency range from 10^5 to 10^{-2} Hz. All the EIS experiments were carried out in 0.01 mol·L^{-1} PBS solution (pH 7.4) containing 0.1 mol·L^{-1} KCl and 5 mmol·L^{-1} $K_3[Fe(CN)_6]/K_4[Fe(CN)_6]$ (1:1 mixture). Fig. 4 shows the impedance spectra of bare GE, γ-PGA/GE, ATh-γ-$PGA_{22.0\%}$/GE, ATh-γ-$PGA_{22.0\%}$/GE after electropolymerization and HRP/ATh-γ-$PGA_{22.0\%}$/GE. Obviously, the bare GE exhibited a small semicircle domain with the value of 120 Ω (R_{ct}). After modified by the γ-PGA, the R_{ct} increased to about 870 Ω. The much larger R_{ct} value than that of the bare GE indicated that γ-PGA modified GE had a large electron transfer resistance. Comparatively, the ATh-γ-$PGA_{22.0\%}$/GE exhibited a smaller semicircle domain with the value of about 480 Ω. However, after electropolymerization, the semicircle was reduced to 80 Ω, which was more than six times lower than the value before electropolymerization. The significantly decrease of R_{ct} demonstrated that the electron transfer between the electrode and electrolyte was accelerated and the conductivity of the NPs film was improved. After immobilization of HRP, the R_{ct} increased to about 550 Ω, suggesting a decrease in conductivity due to the adsorption of non-conductive HRP which hindered electron-transfer.

Fig. S8 shows the morphologies of different modified electrodes. It can be seen from the SEM images that the nanostructured particles morphology in Fig. S8(b) became more homogeneous after electropolymerization (Fig. S8(c)), which can be attributed to the cross-linking of the NPs induced by the electropolymerization. The nanostructured particles morphology of ATh-γ-$PGA_{22.0\%}$ on the electrode after electropolymerization also was confirmed by AFM image (Fig. S8(e)). Fig. S8(d) shows the SEM image of HRP/ATh-γ-$PGA_{22.0\%}$/GE with an obvious changed morphology of the particles, indicating the successful adsorption of HRP on the surface of the ATh-γ-$PGA_{22.0\%}$ NPs film. All these morphologic changes demonstrated the success of stepwise modifications of the GE. After Nafion, which is helpful in protecting the biocompatibility of the enzyme and preventing it from leakage, was cast on the surface of HRP/ATh-γ-

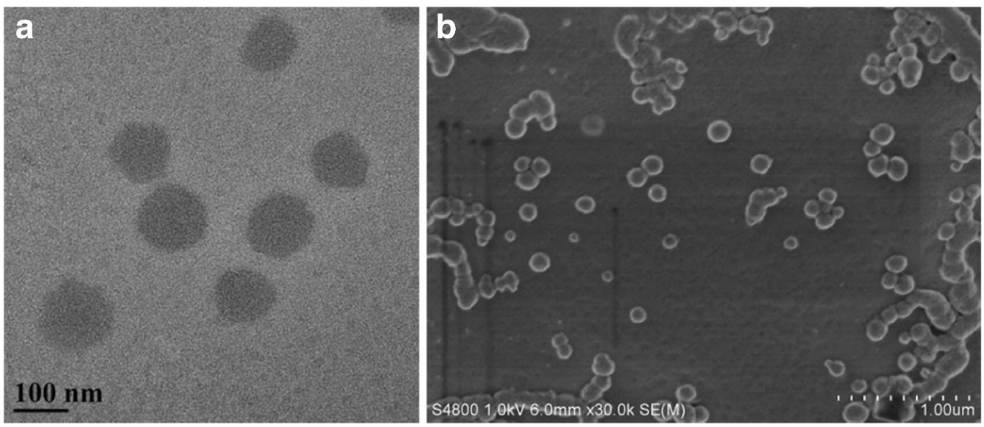

Fig. 3 TEM image (**a**) and SEM image (**b**) of ATh-γ-$PGA_{22.0\%}$ NPs formed in aqueous solution at pH 2.5. The concentration of ATh-γ-$PGA_{22.0\%}$ copolymer in aqueous solution was 0.1 mg·mL^{-1}

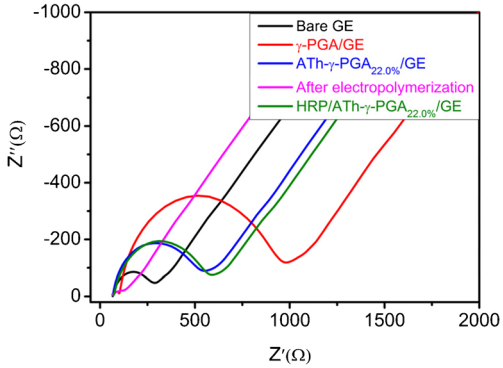

Fig. 4 Nyquist plots corresponding to various modified electrodes. The impedance spectra were recorded at an open-circuit voltage and an AC amplitude of 5 mV over a frequency range from 10^5 to 10^{-2} Hz. The EIS experiments were carried out in 0.01 mol·L^{-1} PBS solution (pH 7.4) containing 0.1 mol·L^{-1} KCl and 5 mmol·L^{-1} $K_3[Fe(CN)_6]/K_4[Fe(CN)_6]$ (1:1 mixture)

$PGA_{22.0\%}$/GE, the electrochemical biosensor Nafion/HRP/ATh-γ-$PGA_{22.0\%}$/GE was fabricated.

Performance of the electrochemical biosensor

The DET between the HRP and the underlying GE can be readily achieved via a high biocompatible system based on ATh-γ-$PGA_{22.0\%}$ NPs. Fig. S9 shows the typical CVs of the Nafion/HRP/γ-PGA/GE, Nafion/ATh-γ-$PGA_{22.0\%}$/GE and Nafion/HRP/ATh-γ-$PGA_{22.0\%}$/GE. Compared with Nafion/HRP/γ-PGA/GE and Nafion/ATh-γ-$PGA_{22.0\%}$/GE, a pair of high and stable redox peaks of HRP in pH 7.0 PBS solution for the HRP (Fe^{III})/HRP (Fe^{II}) redox couple transformation was observed at the Nafion/HRP/ATh-γ-$PGA_{22.0\%}$/GE, which was ascribed to the electron transfer between the HRP and the underlying electrode. Therefore, the conducting ATh-γ-$PGA_{22.0\%}$ NPs were the key factor to enhance the direct electron transfer of HRP.

In order to confirm the concentration of ATh-γ-$PGA_{22.0\%}$ NPs solution for preparing biosensor, 5 μL of different concentrations of ATh-γ-$PGA_{22.0\%}$ NPs solution (0.05, 0.08, 0.10 mg·mL^{-1}) was cast on the surface of GE to fabricate biosensor, respectively. The electrochemical currents of prepared Nafion/HRP/ATh-γ-$PGA_{22.0\%}$/GE in pH 7.0 PBS solution were determined by differential normal pulse voltammetry (DNPV) technique. The scan rate was 20 mV·s^{-1}. The relationship of peak currents subtracted the baseline and the concentration of ATh-γ-$PGA_{22.0\%}$ NPs is shown in Fig. S10. As can be seen, the electrochemical current at 127 V of biosensor prepared from 0.08 mg·mL^{-1} of ATh-γ-$PGA_{22.0\%}$ NPs solution was larger than the biosensors prepared from other concentrations of ATh-γ-$PGA_{22.0\%}$ NPs solution. So, the Nafion/HRP/ATh-γ-$PGA_{22.0\%}$/GE prepared from 0.08 mg·mL^{-1} was used in the following work.

In most cases the redox behavior of HRP is significantly dependent on the pH value of buffer solution. So the influence of buffer pH on properties of biosensor Nafion/HRP/ATh-γ-$PGA_{22.0\%}$/GE was investigated in 0.1 mmol·L^{-1} PBS solution with pH values ranging from 4.0 to 9.0. As shown in Fig. 5, the maximum peak current was occurred at pH 7.0, which was selected for the electrochemical investigation.

Previous republished work reported that HRP exhibited excellent electrocatalytic activity toward H_2O_2. The reaction mechanism [6] of the H_2O_2 biosensor was briefly summarized as below:

$$HRP\left(Fe^{II}\right) + H_2O_2 \rightarrow HRP\left(Fe^{III}\right) + H_2O$$
$$HRP\left(Fe^{III}\right) + e \rightarrow HRP\left(Fe^{II}\right)$$

The DNPV voltammograms of Nafion/HRP/ATh-γ-$PGA_{22.0\%}$/GE in mol·L^{-1} PBS solution (pH 7.0) with different concentrations of H_2O_2 are shown in Fig. 6. It can be seen in Fig. 6a, the DNPV peak currents of the biosensor increased with increasing H_2O_2 concentration and showed linear relationships ranging from 1×10^{-11} to 1×10^{-5} mol·L^{-1}. The calibration curve in Fig. 6b revealed that the peak currents at 127 V were proportional to the concentrations of H_2O_2 in two segments: the first linear segment increased from 1×10^{-11} to 1×10^{-8} mol·L^{-1} with a linear regression equation of $I(\mu A) = 9.142 + 0.271 \times \log C(H_2O_2)$ ($R^2 = 0.999$), and the second linear segment increased from 1×10^{-8} to 1×10^{-5} mol·L^{-1} with a linear regression equation of $I(\mu A) = 8.043 + 0.132 \times \log C(H_2O_2)$ ($R^2 = 0.997$). These results revealed that the resulting Nafion/HRP/ATh-γ-$PGA_{22.0\%}$/GE biosensor in the present work possessed a higher affinity to H_2O_2. This method showed good sensitivity for sensing H_2O_2. The electrochemical sensitivities obtained from corresponding linear regression equation were 0.0384 μA·(log mol·L^{-1})$^{-1}$·cm^{-2} and 0.0187 μA·(log mol·L^{-1})$^{-1}$·cm^{-2}, respectively. Under the same conditions, the response currents for H_2O_2 with different concentrations at the electrode in the absence of HRP (Nafion/ATh-γ-$PGA_{22.0\%}$/GE) have been conducted. The results are

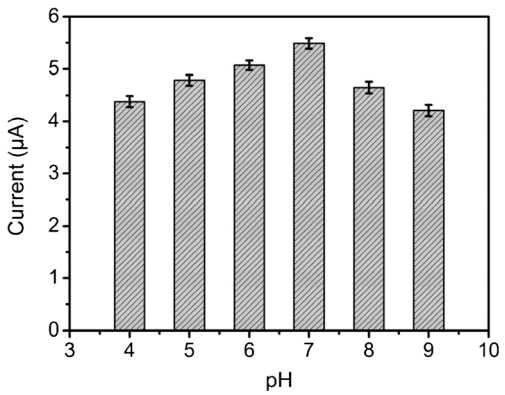

Fig. 5 The peak currents in 0.1 mol·L^{-1} PBS solution with different pH values determined by Nafion/HRP/ATh-γ-$PGA_{22.0\%}$/GE biosensors

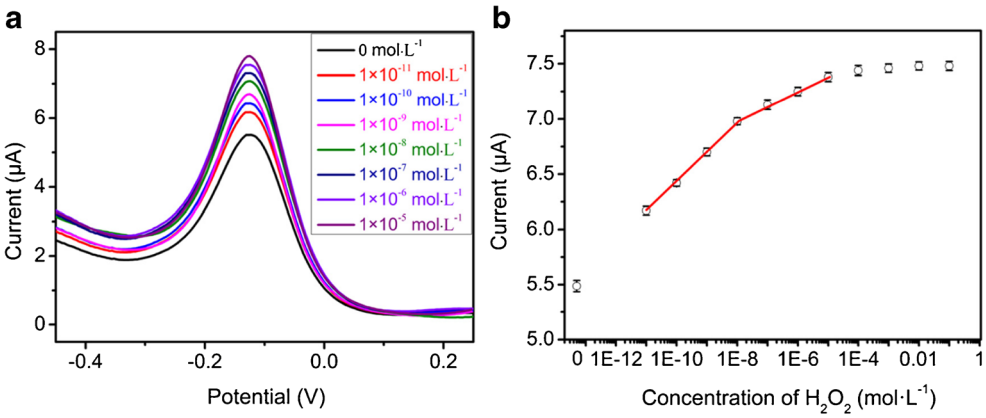

Fig. 6 (**a**) Differential normal pulse voltammograms of H_2O_2 with different concentrations at Nafion/HRP/ATh-γ-$PGA_{22.0\%}$/GE in 0.1 mol·L^{-1} PBS solution (pH 7.0). The scan rate is 20 mV·s^{-1}. (**b**) Calibration curves corresponding to the response recorded on the Nafion/HRP/ATh-γ-$PGA_{22.0\%}$/GE biosensor versus the concentration of H_2O_2

shown in Fig. S11. As can be seen that compared with Nafion/HRP/ATh-γ-$PGA_{22.0\%}$/GE, the response currents of the Nafion/ATh-γ-$PGA_{22.0\%}$/GE for H_2O_2 were independent of the concentration, and stayed at very low values for all the concentrations within the test range.

Additionally, we did a comparison of our prepared Nafion/HRP/ATh-γ-$PGA_{22.0\%}$/GE biosensor with other previously reported biosensors for sensing H_2O_2. As can be seen in Table. 1, our prepared Nafion/HRP/ATh-γ-$PGA_{22.0\%}$/GE biosensor exhibited much wider detection range with lower detection limit for sensing H_2O_2 than other biosensors in the previous reports. The wider detection range with lower detection limit was attributed to the large specific surface area of the nanosized ATh-γ-$PGA_{22.0\%}$ NPs-based film, which can immobilize a great number of HRP with high surface-to volume ratio. In addition, the electropolymerization of thiophene moieties formed a cross conjugated conductive polymer network, which accelerated the electron transfer and facilitated the signal transduction from the enzyme to the underlying electrode, resulting in the increase of sensitivity of Nafion/HRP/ATh-γ-$PGA_{22.0\%}$/GE biosensor .

To investigate the reproducibility of the Nafion/HRP/ATh-γ-$PGA_{22.0\%}$/GE biosensor, four biosensors were constructed under identical experimental conditions. For detecting H_2O_2 of 1×10^{-10} mol·L^{-1} in 0.1 mol·L^{-1} PBS solution (pH 7.0), the peak current at 127 V was determined by using each of Nafion/HRP/ATh-γ-$PGA_{22.0\%}$/GE biosensor. The results are shown in Fig. S12. It can be seen that the standard deviation of the response did not exceed 3%, indicating that the prepared biosensor exhibited excellent reproducibility.

The stability of the Nafion/HRP/ATh-γ-$PGA_{22.0\%}$/GE biosensor was also investigated through sensing 1×10^{-10} mol·

Table 1 Comparison of the sensing performance of our biosensor with previously reported H_2O_2 electrochemical biosensors

Biosensor[a]	Linear range (mol·L^{-1})	Detection limit (mol·L^{-1})	References
Nafion/HRP/ATh-γ-$PGA_{22.0\%}$/GE	1×10^{-11} – 1×10^{-8} 1×10^{-8} – 1×10^{-5}	3×10^{-12}	Present work
Nafion/Hb/PPy-C_{60}-DDAB/CILE	1×10^{-6}–1.141×10^{-4} 1.141×10^{-4}–1.479×10^{-3}	3×10^{-7}	[28]
HRP/PANI/PVS modified electrode	1×10^{-5}–6×10^{-4} 1×10^{-3}–6×10^{-2}	–	[29]
Amplex Red-mediated SWV, soluble HRP	8×10^{-12}–3×10^{-10} 3×10^{-10}–3×10^{-6}	8×10^{-13} 3×10^{-11}	[30]
Amplex Red-mediated SWV, immobilized HRP	2×10^{-9}–5×10^{-8}	2×10^{-9}	
NAD^+-SWCNTs modified GCE	1×10^{-10} – 1×10^{-7}	1×10^{-11}	[31]
$Cu_2(OH)_3Cl$-CeO_2 composite material	2×10^{-5} – 5×10^{-5}	1×10^{-5}	[32]
BD-ROM electrode	2.5×10^{-3} – 10×10^{-2}	6×10^{-3}	[33]
PEDOT/PB modified electrode	5×10^{-7} – 8.39×10^{-4}	1.6×10^{-7}	[34]
Nafion/HRP/IP_6/GCE	1×10^{-7}–5×10^{-7} 6×10^{-7}–1.6×10^{-6}	1×10^{-7}	[6]

[a] Abbreviations: *PPy-C_{60}-DDAB* polypyrrole-fullerene-didodecyldimethylammonium bromide, *CILE* carbon ionic liquid electrode, *PANI* polyaniline, *PVS* poly-vinylsulphonic acid, *SWV* Square wave voltammetry, *NAD^+* nicotinamide adenine dinucleotide ion, *GCE* glassy carbon electrode, *SWCNTs* single walled carbon nanotubes, *BD-ROM* blu-ray disc-read only memory, *PEDOT* poly(3,4-ethylenedioxythiophene), *PB* Prussian blue, *IP_6* botanical inositol hexakisphosphoric

L^{-1} H_2O_2 in 0.1 mol·L^{-1} PBS solution (pH 7.0). The results are shown in Fig. S13. The calculated RSD was about 2.4% ($n = 8$). The biosensor can retain its property for 4 weeks as it was stored in air at room temperature, indicating that the Nafion/HRP/ATh-γ-$PGA_{22.0\%}$/GE biosensor response was quite stable. The peak current at 127 V upon interaction with 1×10^{-10} mol·L^{-1} H_2O_2 in 0.1 mol·L^{-1} PBS solution (pH 7.0) decreased by about 30% after 1 month of storage.

To assess the applicability of resultant Nafion/HRP/ATh-γ-$PGA_{22.0\%}$/GE, the biosensor was applied to detect the concentration of H_2O_2 in commercial disinfector. The sample was diluted 10,000,000-fold with 0.1 mol·L^{-1} PBS solution (pH 7.0). The average concentration of H_2O_2 in sample was 9.83 mol·L^{-1} determined by the Nafion/HRP/ATh-γ-$PGA_{22.0\%}$/GE for four assays as shown in Tab. S2. Using the potassium permanganate titration method, the concentration of H_2O_2 in sample was measured to be 9.79 mol·L^{-1}. The relative standard deviation of results obtained by two measurements was 2%, indicating that it was practicable to apply the Nafion/HRP/ATh-γ-$PGA_{22.0\%}$/GE biosensor to determine H_2O_2 in medicine sample.

In addition, the interference study was carried out by measuring the biosensor response before and after addition of some interferent (ascorbic acid, dopamine, glucose, and l-cysteine) into the 0.1 mol·L^{-1} PBS solution containing 1×10^{-10} mol·L^{-1} H_2O_2 at their physiological concentration [35]. The peak currents in 0.1 mol·L^{-1} PBS solution (pH 7.0) containing H_2O_2 of 1×10^{-10} before and after addition of interferent at Nafion/HRP/ATh-γ-$PGA_{22.0\%}$/GE biosensors determined by DNPV are shown in Fig. S14. The results revealed that the addition of relevant physiological concentrations of interferent did not reveal obvious additional signals, suggesting good selectivity of the prepared biosensor.

Conclusion

In this work, a conducting nanoparticles-based film consisting of ATh-γ-PGA was prepared by macromolecular self-assembly and electropolymerization. The prepared Nafion/HRP/ATh-γ-$PGA_{22.0\%}$/GE biosensor increased with increasing H_2O_2 concentration and showed linear relationships ranging from 1×10^{-11} to 1×10^{-5} mol·L^{-1} in two segments with low detection limit and high sensitivity. Good selectivity and repeatability of the prepared biosensor were also demonstrated. The prepared biosensor also exhibited good stability within 1 month of storage. After 5 weeks of storage, the electrochemical response current for H_2O_2 significantly decreased. As a practical application, the fabricated biosensor was successfully and accurately employed to detect the amount of H_2O_2 presented in commercial disinfector with satisfactory results.

Acknowledgements This work was supported by the National Natural Science Foundation of China (NSFC 21504001, 51572004), the foundation of Key Laboratory of Food Colloids and Biotechnology, Ministry of Education, Jiangnan University (JDSJ2015-02), Natural Science Foundation of the Higher Education Institutions of Anhui Province (KJ2016SD06, KJ2017A115) and the Anhui Provincial Natural Science Research Program of High Education Improvement Plan (TSKJ2016B17).

Compliance with ethical standards The author(s) declare that they have no competing interests.

References

1. Chen W, Cai S, Ren QQ, Wen W, Zhao YD (2012) Recent advances in electrochemical sensing for hydrogen peroxide: a review. Analyst 137:49–58
2. Liu Q, Lu XB, Li J, Yao X, Li JH (2007) Direct electrochemistry of glucose oxidase and electrochemical biosensing of glucose on quantum dots/carbon nanotubes electrodes. Biosens Bioelectron 22:3203–3209
3. Li J, Lin XQ (2007) Glucose biosensor based on immobilization of glucose oxidase in poly(o-aminophenol) film on polypyrrole-Pt nanocomposite modified glassy carbon electrode. Biosens Bioelectron 22:2898–2905
4. Xu Q, Zhu JJ, Hu XY (2007) Ordered mesoporous polyaniline film as a new matrix for enzyme immobilization and biosensor construction. Anal Chim Acta 597:151–156
5. Wang L, Wang EK (2004) A novel hydrogen peroxide sensor based on horseradish peroxidase immobilized on colloidal Au modified ITO electrode. Electrochem Commun 6:225–229
6. Miao Y, Wen Y, Dong J, Zhou WX, Zhang ZR, Yang HF (2011) Botanical micelle and its application for direct electrochemical biosensor. Biosens Bioelectron 26:2994–2999
7. Gorton L, Lindgren A, Larsson T, Munteanu FD, Ruzgas T, Gazaryan I (1999) Direct electron transfer between heme-containing enzymes and electrodes as basis for third generation biosensors. Anal Chim Acta 400:91–108
8. Jia JB, Wang BQ, AG W, Cheng GJ, Li Z, Dong SJ (2002) A method to construct a third-generation horseradish peroxidase biosensor: self-assembling gold nanoparticles to three-dimensional sol-gel network. Anal Chem 74:2217–2223
9. Mukhopadhyay P, Mishra R, Rana D, Kundu PP (2012) Strategies for effective oral insulin delivery with modified chitosan nanoparticles: a review. Prog Polym Sci 37:1457–1475
10. Yang YQ, Luo J, Liu R, Liu JK, Jiang JQ, Liu XY (2011) Glucose sensors based on electrodeposition of molecularly imprinted polymeric micelles: a novel strategy for MIP sensors. Biosens Bioelectron 26:2607–2612
11. Luo J, Fan CH, Wang XH, Liu R, Liu XY (2013) A novel electrochemical sensor for paracetamol based on molecularly imprinted polymeric micelles. Sensors Actuators B Chem 188:909–916
12. Zhang RL, Xu S, Luo J, Shi DJ, Liu C, Liu XY (2014) One-pot green synthesis of nanohybrid structures: gold nanoparticles in poly(γ-glutamic acid) copolymer nanoparticles. RSC Adv 4: 25106–25113
13. Zhang RL, Xu S, Zhu Y, Zhao W, Luo J, Liu XY, Tang DX (2016) Molecularly imprinted nanohybrids based on dopamine-modified poly(γ-glutamic acid) for electrochemical sensing of melamine. Biosens Bioelectron 85:381–386
14. Zhang RL, Xu S, Luo J, Liu XY (2015) Molecularly imprinted photo-sensitive polyglutamic acid nanoparticles for electrochemical sensing of hemoglobin. Microchim Acta 182:175–183

15. Zhang RL, Sun JD, Luo J, Xu S, Liu XY (2014) Preparation of photo-sensitive poly(γ-glutamic acid) nanoparticles and application for immobilizing hemoglobin on electrode. Colloid Polym Sci 292: 2295–2302
16. Ates M (2013) A review study of (bio)sensor systems based on conducting polymers. Mater Sci Eng C 33:1853–1859
17. Aguilar-Ortíz E, Zaragoza-Galán G, Solladié N, Rein R, Aguilar-Martínez M, Macías-Ruvalcaba N, Rivera E (2012) Preparation and characterization of novel polythiophenes bearing oligo(ethylene glycol) spacers and porphyrin units: optical and electrochemical properties. Synth Met 2162:1000–1009
18. Nien PC, Chen PY, Ho KC (2009) Fabricating an amperometric cholesterol biosensor by a vovalent linkage between poly(3-thiopheneacetic acid) and cholesterol oxidase. Sensors 9:1794–1806
19. Xu J, Bai HY, Yi CL, Luo J, Yang C, Xia WS, Liu XY (2011) Self-assembly behavior between native hyaluronan and styrylpyridinium in aqueous solution. Carbohydr Polym 86:678–683
20. Luo J, Ma Q, Wei W, Zhu Y, Liu R, Liu XY (2016) Synthesis of water-dispersible molecularly imprinted electroactive nanoparticles for the sensitive and selective paracetamol detection. ACS Appl Mater Interfaces 8:21028–21038
21. Krikstolaityte V, Kuliesius J, Ramanaviciene A, Mikoliunaite L, Kausaite-Minkstimiene A, Oztekin Y, Ramanavicius A (2014) Enzymatic polymerization of polythiophene by immobilized glucose oxidase. Polymer 55:1613–1620
22. Pal RK, Farghaly AA, Wang CZ, Collinson MM, Kundu SC, Yadavalli VK (2016) Conducting polymer-silk biocomposites for flexible and biodegradable electrochemical sensors. Biosens Bioelectron 81:294–302
23. Lei W, Si WM, Xu YJ, Gu ZY, Hao QL (2014) Conducting polymer composites with graphene for use in chemical sensors and biosensors. Microchim Acta 181:707–722
24. Zhang HQ, Hu LW, Tu JG, Jiao SQ (2014) Electrochemically assembling of polythiophene film in ionic liquids (ILs) microemulsions and its application in an electrochemical capacitor. Electrochim Acta 120:122–127
25. Pang YH, Li XY, Ding HL, Shi GY, Jin LT (2007) Electropolymerization of high quality electrochromic poly(3-alkylthiophene)s via a room temperature ionic liquid. Electrochim Acta 52:6172–6177
26. Fei XM, Luo J, Liu R, Liu JC, Liu XY, Chen MQ (2015) Multiwalled carbon nanotubes noncovalently functionalized by electro-active amphiphilic copolymer micelles for selective dopamine detection. RSC Adv 5:18233–18241
27. Prodromidis MI (2010) Impedimetric immunosensors-a review. Electrochim Acta 55:4227–4233
28. Dong Y, Wang L, Nie F, Zheng JB (2016) Hydrogen peroxide biosensor based on polypyrrole-pullerene-DDAB nanocomposite film. Sens Lett 14:656–664
29. Sun MJ, Song GQ, Liu JJ, Chen HM, Nie FQ (2017) *In situ* controllable synthesis of cotton-like polyaniline nanostructures for a H_2O_2 sensor using an embedded three-electrode microfluidic chip. RSC Adv 22:13637–13642
30. Lyon JL, Stevenson KJ (2006) Picomolar peroxide detection using a chemically activated redox mediator and square wave voltammetry. Anal Chem 78:8518–8525
31. Salimi A, Miranzadeh L, Hallaj R, Mamkhezri H (2008) Picomolar detection of hydrogen peroxide at glassy carbon electrode modified with NAD^+ and single walled carbon nanotubes. Electroanalysis 20:1760–1768
32. Wang N, Sun JC, Chen LJ, Fan H, Ai SY (2015) A $Cu_2(OH)_3Cl$-CeO_2 nanocomposite with peroxidase-like activity, and its application to the determination of hydrogen peroxide, glucose and cholesterol. Microchim Acta 182:1733–1738
33. Ngamaroonchote A, Chotsuwan C, Tantisantisom K, Laocharoensuk R (2017) Patterned gold electrode prepared from optical discs display largely enhanced electrochemical sensitivity as exemplified in a sensor for hydrogen peroxide. Microchim Acta 184:211–218
34. Wang JJ, Wang Y, Cui M, Xu SH, Luo XL (2017) Enzymeless voltammetric hydrogen peroxide sensor based on the use of PEDOT doped with Prussian blue nanoparticles. Microchim Acta 184:483–489
35. Lata S, Batra B, Karwasra N, Pundir CS (2012) An amperometric H_2O_2 biosensor based on cytochrome c immobilized onto nickel oxide nanoparticles/carboxylated multiwalled carbon nanotubes/polyaniline modified gold electrode. Process Biochem 47:992–998